Nonradiative and dissociative decay channels of core-excited H_2S studied by *ab initio* calculations

Arnaldo Naves de Brito
MAX-Laboratory, University of Lund, Box 118, S-221 00 Lund, Sweden

Hans Ågren
Institute of Quantum Chemistry, University of Uppsala, Box 518, S-75120 Uppsala, Sweden
(Received 13 August 1991)

Ab initio studies of the $2p(3a_1)$-$6a_1$ and $2p(3a_1)$-$3b_2$ photoexcitation resonances of H_2S have been carried out in order to support interpretations of recent photoelectron and autoionization spectra using synchrotron-radiation excitation. The full $H_2S^* \rightarrow S+H_2$ and $H_2S^* \rightarrow S+H+H$ potential-energy surfaces as well as the resonant energies for autoionization (Auger) decay of core-excited states in the fragment HS species have been obtained by multiconfiguration self-consistent-field calculations. The results support an interpretation of the spectral fundings in terms of fast dissociation of the H_2S^* $2p^{-1}6a_1^1$ and $2p^{-1}3b_2^1$ states to core-excited states in HS^* followed by resonance Auger decay to HS^+ valence single-hole states.

PACS number(s): 33.80.Eh, 32.80.Hd, 31.20.Di, 33.80.Gj

I. INTRODUCTION

Due to the possibility of obtaining high-quality spectra from synchrotron radiation with tunable excitation energies and narrow bandwidths there has lately been a resurgent interest in resonance Auger spectroscopy of small molecules. The interpretation of such spectra generally calls for theoretical considerations that go beyond those of Auger spectra emanating from core-hole states. These considerations relate to interference effects among the electronic decay channels as well as to fast dissociation of the core-excited states that are initial of the resonant decay. The latter mechanism has found support by the fact that, while higher excited states involving Rydberg levels show sharp photoexcitation lines, the states filling empty valencelike orbitals are often much broader than the natural widths of the core-hole states. Furthermore, the nonradiative decay of the latter states show spectra that are not easily interpretable in terms of diagram levels of the compound molecule. Rather, excitation energy dependencies as well as findings by mass spectroscopy have indicated a mechanism in which dissociation is faster than the electronic decay of the excited fragment.

The hydrides have particular properties that motivate interpretation of their resonance Auger spectra in terms of fast dissociation. This kind of decay channel was first identified in the photoelectron spectrum of HBr recorded at the $3d \rightarrow \sigma^*$ excitation energy [1]. The HCl $2p \rightarrow \sigma^*$ resonance was also found to decay predominantly by the dissociation followed by the electronic decay [2]. The time scales of the dissociation and the Auger decay were found to be of the same order of magnitude. In contrast to the model used in the HBr case [1] the work on HCl [2] predicted the simultaneous existence of molecular and atomic Auger spectra. Very recently, corresponding resonance Auger spectra was recorded for H_2S with high resolution at resonance photon energies (Aksela *et al.* [3], hereafter denoted as paper I).

To explore if "dissociation before decay" is possible one has to investigate the kinematic and dynamic aspects in detail, solving the quantum equations of motions in the multidimensional potential-energy surface (PES). Although some of the formal equations associated to this have been addressed lately [4,5], a full numerical account is laborious. In this work we explore Auger resonance decay of core-excited H_2S from the energetic and topological points of view, by making PES and spectroscopic calculations for the decay channels of the core-excited H_2S. The PES's are obtained for the ground state and selected excited states of H_2S using the complete active space self-consistent field method. H_2S is isoelectronic with the recently studied argon and HCl species, but, being three-atomic, provides the intrinsic complication of dissociating through more than one channel and the possibility of distributing excess electronic energy into both external and internal degrees of freedom for the nuclear motions. The channels we investigate can be summarized as the following.

(i) Fast dissociation of both hydrogens into (a) separated atoms and (b) the H_2 molecule, followed by the Auger process in the excited sulfur atom, hereafter referred to as channels 1a and 1b, respectively (also denoted as channel 1 when the product of the hydrogen dissociation is not important for the discussion).

(ii) Dissociation of one hydrogen followed by the Auger process in the excited HS molecule (channel 2).
An additional channel can be described.

(iii) Auger decay in the excited H_2S molecule before dissociation (channel 3).

Channel 3 as well as channels 1 and 2 are investigated in the companion paper [3] basing on experimental evidence.

II. THEORETICAL METHOD

The potential-energy surfaces for the ground-state core-excited $3a_1^{-1}6a_1^1$ and $3a_1^{-1}3b_2^1$ states of H_2S were

calculated by the multiconfiguration self-consistent-field (MCSCF) method using complete active space wave functions. The calculations for the H_2S ground state $1a_1^2 2a_1^2 3a_1^2 1b_2^2 1b_1^2 4a_1^2 2b_2^2 5a_1^2 2b_1^2$ were performed using the $1a_1$, $2a_1$, $3a_1$, $1b_2$, and $1b_1$ orbitals as inactive (doubly occupied), and the $4a_1$, $2b_2$, $5a_1$, $2b_1$, $6a_1$, $3b_2$, $7a_1$, $3b_1$, and $1a_2$ orbitals as active [fractionally occupied and determining complete configuration-interaction (CI) distributions]. For the $3a_1^{-1}6a_1^1$ and $3a_1^{-1}3b_2^1$ excited states the $3a_1$ orbital was kept singly occupied. The calculations for the HS molecule were performed by dividing the orbital space in such a way that the 1σ, 2σ, 3σ, and 1π orbitals were inactive and the 4σ, 2π, 5σ, 6σ, 3π, and 1δ orbitals were active. This choice was made to match the orbital division for H_2S, thus obtaining comparable energies. The choice of the active spaces was guided by natural orbital occupation analysis from a Møller-Plesset second-order perturbation calculation (MP2) on the ground state. Test calculations with the restricted active space (RAS) method was also performed at selected points. The possible variation of the natural orbital occupation for different geometries at the MP2 level was also studied for the ground state and no major change of this occupation was observed. All calculations were performed with the SIRIUS/ABACUS code for MCSCF wave functions and properties [6,7]. Global PES's were obtained by selection of a grid of points. A few searches of the PES's were also conducted by using the analytical gradient and Hessians (ABACUS code).

The grids for the PES calculations were obtained by varying the internuclear bond distance between sulfur and hydrogen atoms from 1 to 10 a.u. Potential-energy curves were calculated for three internuclear bond angles 91.96°, 135°, and 180°. The 91.96° angle and the interatomic distance of 2.53 a.u. are the equilibrium values for neutral H_2S molecules in the ground state calculated with the same active space as given above [8]. Calculations for the neutral excited ($3a_1^{-1}6a_1^1$) and ($3a_1^{-1}3b_2^1$) states of H_2S show that both the basis set (described below) and the active space provide good descriptions for these states.

Figure 1 shows the points calculated on the energy surface. Channels 1a and 2 together with a representation of the molecular geometry of the dissociation limits are also indicated in the figure for further reference. In order to make the energy surface plots we performed a bidimensional spline interpolation procedure in the calculated mesh [7]. A more dense mesh of points was calculated in the direction of channels 1a and 2 in order to obtain a better description of the curve in this direction. It should be noticed that the potential-energy surface has a symmetry plane through channel 1a.

Fast dissociation of H_2S into the H_2 molecule and excited sulfur atom, channel 1b, was also studied by calculating the PES surfaces for the $3a_1^{-1}6a_1^1$ and $3a_1^{-1}3b_2^1$ states for closing interatomic angles of H_2S. We calculate the PES with the hydrogens in symmetric positions at three different S-H interatomic distances: 2.53, 2.75, and 3.00 a.u. We started with an interatomic H-H distance of 4.2 a.u. and decreased it in steps of 0.28 to 1.4 a.u., which

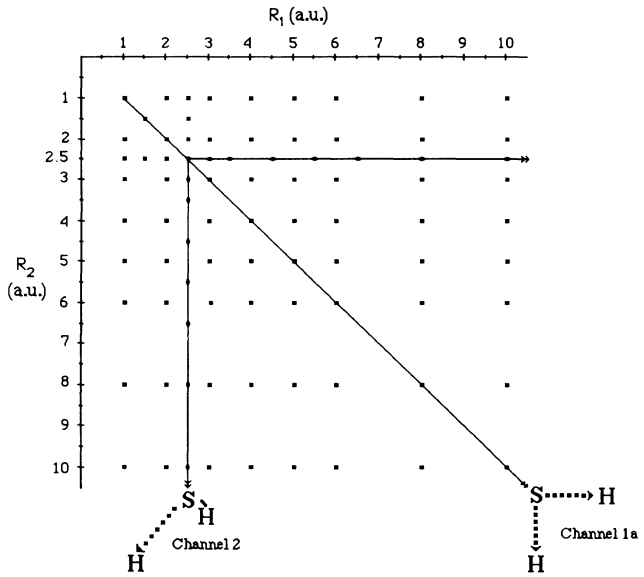

FIG. 1. The grid of points for PES calculations at fixed bond angles. The solid lines represent the channels. Resulting dissociation products are indicated.

is the H_2 ground-state equilibrium distance.

The PES's of the $3a_1^{-1}6a_1^1$ and $3a_1^{-1}3b_2^1$ states were calculated using a frozen $3a_1$ orbital. For the equilibrium geometry a relaxed energy of the core orbital of only 0.21 eV was obtained. The core-relaxed potential-energy surface is expected to be parallel to the frozen core surface because the effect of charge penetration from the hydrogens into the core is minor.

For all the excited states only the excitation from the $3a_1$ and 3σ orbitals of H_2S and HS, respectively, was considered. The excitations from the S $2p$ $1b_1$ and $1b_2$ orbitals were not considered because the energy difference of the $1b_1^{-1}$ and $1b_2^{-1}$ levels caused by molecular symmetry, if any, is less than 0.1 eV [8], and is negligible compared to the spin-orbit splitting of 1.2 eV. This molecular-field splitting may thus only cause some minor broadening of the observed spectral peaks.

The basis set used here and employed by Cesar *et al.* [8] for calculations of normal Auger spectra of H_2S has previously also been advocated by Roos and Siegbahn [10] (*d* functions), Strömberg *et al.* [11], and by Magnusson and Schaefer [12] in other contexts. It has the following compositions: a ($4s$) Veillard basis set for hydrogen contracted to a [$3s$] and argumented with one polarization function $p(\alpha=0.8)$; a Veillard ($12s9p$) basis set for sulfur contracted according to Dunning to [$7s4p$]; and two *d* functions ($\alpha=0.54,0.15$) and two diffuse functions with the coefficients given by [$s(\alpha=0.056\,811)$,$p(\alpha=0.036\,266)$].

III. DISCUSSION

A. Potential-energy studies of HS+H and S+H+H

Figures 2(a)–2(c) show the potential-energy surfaces calculated for ground-state first ($3a_1 \rightarrow 6a_1$) and second

$(3a_1 \rightarrow 3b_2)$ core-excited states, respectively. The bond angle is fixed to 91.96°, which is the ground-state equilibrium bond angle. In these figures the interatomic distance varies from 2 to 8 a.u. and each division in the plot corresponds to 0.125 a.u. In the discussion of Figs. 2–4 channels 1a and 2 have the same meaning as shown in Fig. 1.

1. Ground $^1A_1$ state

For the PES of the ground state, Fig. 2(a), channel 2 shows up with a transition state, while channel 1a is completely closed. In the direction of channel 2 the dissociation limit corresponds to $H(1s^1)^2S + HS(1\sigma^2 2\sigma^2 3\sigma^2 1\pi^4 4\sigma^2 5\sigma^2 2\pi^3)^2\Pi$, the latter being bound. In the direction of channel 1a the dissociation products $[H(1s^1)+H(1s^1)]^3S + S(1s^2 2s^2 2p^6 3s^2 3p^4)^3P$ are found.

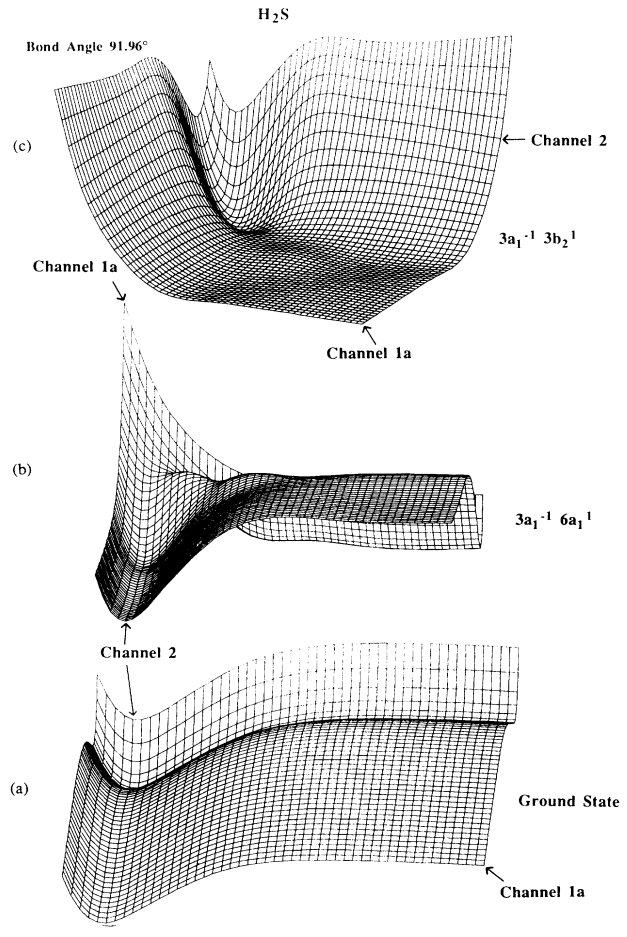

FIG. 2. Graphical representations of the PES's for the ground state, first, and second core-excited states at the equilibrium bond angle. Channels 2 and 1a are indicated. The strong dissociative character of H_2S in the $3a_1^{-1}6a_1^1$ state provides the condition for a fast dissociation into $HS^* + H$ before the Auger decay. See text for futher discussion.

2. Core-excited $^1A_1$ state

Figure 2(b) shows that for the $3a_1^{-1}6a_1^1$ excited state channel 2 has a strong dissociative character. The orbital composition of the dominant configuration and the natural occupancies obtained for the excited $3a_1^{-1}6a_1^1$ state lead to the conclusion that the dissociation gives $HS^* + H$ with the excited HS molecule being in a $(1\sigma^2 2\sigma^2 3\sigma^1 1\pi^4 4\sigma^2 5\sigma^2 2\pi^4)^2\Sigma^+$ state. Again, the resulting HS state is bound. The HS potential well is clearly deeper than that obtained for the ground state. We conclude that the hydrogen sulfide fragment will remain stable with no further dissociation. No dissociation character is found in the direction of channel 1a. The dissociation of both hydrogens seems not to be possible in this case since the excitation from the ground state reaches a position close to the potential well minimum in the direction of channel 1a. However, following the dissociation limit of channel 1a, molecular-orbital analysis and energy considerations give the products of the dissociation to be $[H(1s^1)+H(1s^1)]^3S + S(1s^2 2s^2 2p^5 3s^2 3p^5)^3D$.

Around the point where the vertical excitation from the ground state reaches the $3a_1^{-1}6a_1^1$ state there is a clear distortion in the potential curve, see Fig. 2(b). This distortion is due to the interaction between the $3a_1^{-1}6a_1^1$ and $3a_1^{-1}3b_2^1$ states because of the crossing of these two potential curves at the vertical point. Thus the presence of this crossing implies that the excitation from the ground state to the second excited state $3a_1^{-1}3b_2^1$ will also give rise to dissociation of one hydrogen through the crossing even if the $3a_1^{-1}3b_2^1$ PES itself does not show any dissociative channel. At the point where the vertical excitation from the ground state reaches this curve a shallow minimum is found.

3. Core-excited $^1B_2$ state

Neither channel 1a nor channel 2 present dissociative character for the $3a_1^{-1}3b_2^1$ state. If we follow the dissociation limit of channel 2 the following products are found: $H(1s^1)^2S$ plus HS in the configuration $1\sigma^2 2\sigma^2 3\sigma^1 1\pi^4 4\sigma^2 5\sigma^2 2\pi^3 6\sigma^1$ and the state $^2\Pi$. We denote R_1 as the interatomic distance between one of the hydrogens and the sulfur atom and R_2 the distance for the other hydrogen. We can then define a "HS curve" as the curve corresponding to different values of R_2 when R_1 equals 8 a.u. Following the HS curve in Fig. 2(c) one can see that the HS $3\sigma^{-1}6\sigma^1$ state is strongly dissociative. This behavior can be understood by noticing that the $3\sigma^{-1}6\sigma^1$ state corresponds to the photon excitation of one electron from the 3σ core orbital to the antibonding 6σ orbital. By contrast, the HS nondissociative $(3\sigma^{-1}2\pi^4)^2\Sigma$ (a product of dissociation in the first core-excited state in H_2S) corresponds to a promotion of one electron from 3σ to the nonbonding lone pair 2π orbital. The HS $3\sigma^{-1}6\sigma^1$ state can be compared to the same core-excited $3\sigma^{-1}6\sigma^1$ state in HCl [2]. In HCl this state also shows dissociative character, although the HS state is more strongly dissociative. The dissociative product following channel 1a in Fig. 2(c) is $[H(1s^1)+H(1s^1)]^3S$ plus $S(1s^2 2s^2 2p^5 3s^2 3p^5)^3P$.

4. Bond angle 135°

Until now we have considered potential-energy surfaces for the equilibrium bond angle 91.96°. For a more complete analysis, the potential-energy surface at different bond angles has to be investigated. Figure 3 shows the potential-energy surface of the ground state first and second core-excited states for the bond angle equal to 135°. No new features can be identified in the potential curve for the ground state compared to that shown in Fig. 2(a). On the other hand, the first core-excited state $3a_1^{-1}6a_1^1$, Fig. 3(b), shows no signs of crossing with the $3a_1^{-1}3b_2^1$. Channel 2 is still strongly dissociative. In the direction of channel 1a dissociation of both hydrogens seems to be more unlikely since the potential well in this direction is deeper than in the PES at 91.96°. The second excited state, shown in Fig. 3(c), presents some dissociative character in the direction of channel 1a. However, at the ground-state equilibrium geometry one can easily see that the energy of this state is higher at 135° than at 91.96°, shown in Fig. 2(c). This fact corroborates with the finding that the first and second excited states do not cross at 135°.

5. Bond angle 180°

At 180°, Fig. 4(a), other dissociative limits are attained for channels 1a and 2 than at 91.96° and 135°. This is so because while at the two last-mentioned bond angles we have avoided crossing of the ground state and the first uv excited state, at 180° this first uv state has a different symmetry than the ground state, thus dissociation is achieved through avoided crossing with another uv excited state. Channel 2 gives $SH(^2\Sigma^+)+H(^2S)$, while channel 1a gives $S(^1D)+[H+H](^1S)$.

In the potential surface shown in Fig. 5(a) there is a noticeable potential barrier in the direction of channel 2 and channel 1a. These curves represent the H_2S at $180°-\epsilon$ with $\epsilon\rightarrow 0$. This surface shows clearly the avoided crossing between the two $^1A_1$ states in the direction of channel 2. Channel 1a also shows sign of crossing. The dissociative limits are the same as for 91.96° and 135° as expected.

Figure 4(b) shows the corresponding potential surface for $3a_1^{-1}6a_1^1$ at 180°. This surface is very similar to that at 135°. No sign of crossing with the second core-excited state could be found. In the same way the higher symmetry $D_{2\infty}$ at 180° does not introduce any new feature. We

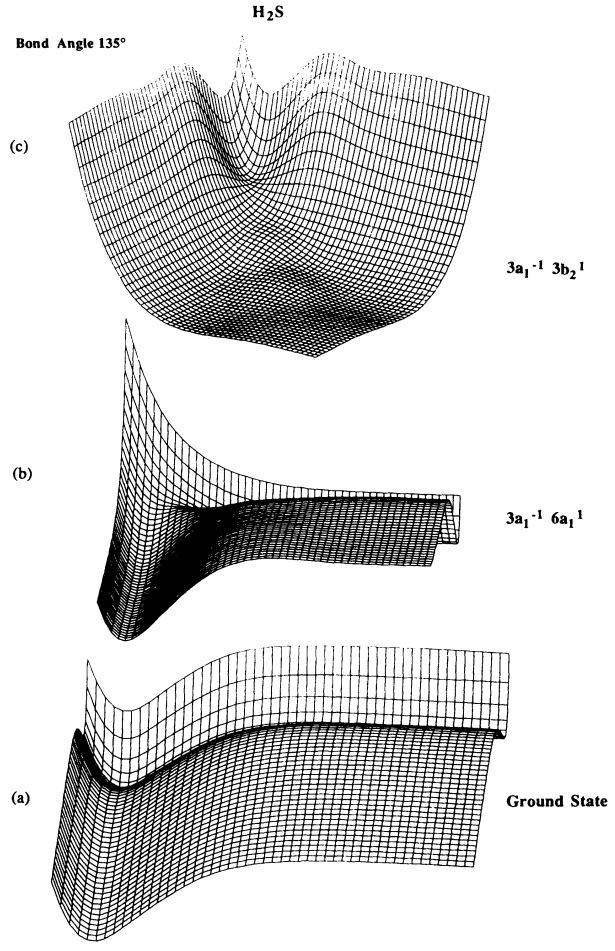

FIG. 3. PES for the ground state and the first two core-excited states at 135°.

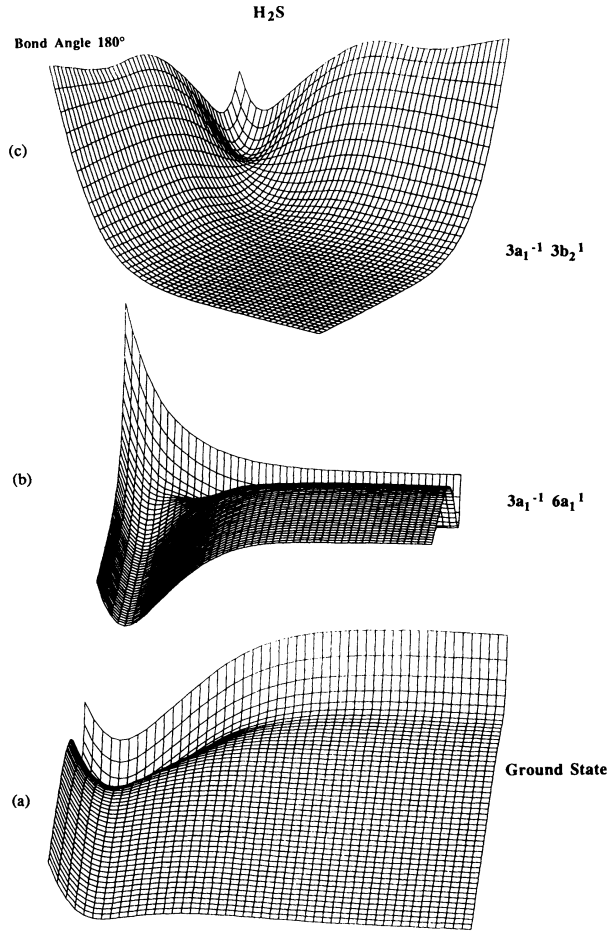

FIG. 4. PES's for the ground state and the first two core-excited states at linear geometry.

will now look closer at the dissociation in both channels 1a and 2. Channel 2 at the excitation point has the configuration $(\cdots 3a_1^{-1}\cdots 2b_2^2 5a_1^2 2b_1^2 6a_1^1 7a_1^0)^1A_1$. After dissociation the $6a_1^1$ localizes to the hydrogen, while the others remain in the HS species. Channel 1a leads to dissociation of hydrogen through a crossing with the state $(\cdots 3a_1^{-1}\cdots 2b_2^2 5a_1^1 2b_1^2 6a_1^1 7a_1^1)^1A_1$. At 180° these two states can be labeled as $(\cdots 1b_{1u}^1\cdots 2b_{1u}^2 2b_{2u}^2 2b_{3u}^2 4a_{1g}^1 3b_{1u}^0)^1B_{1u}$ and $(\cdots 1b_{1u}^1\cdots 2b_{1u}^1 2b_{2u}^2 2b_{3u}^2 4a_{1g}^1 3b_{1u}^1)^1B_{1u}$. As can also be seen at this angle the two crossing states have the same symmetry, therefore unlike the ground state no new restrictions were introduced.

Figures 4(c) and 5(b) show the second excited state at 180° and $180°-\epsilon$. As for the ground state, the linear geometry eliminates the possibility of crossing between some states. Channel 2 in Fig. 4(c) dissociates to HS $(\cdots 3\sigma^1\cdots 5\sigma^1\cdots 6\sigma^1)^2\Sigma^+$, in Fig. 5(b) the same dissociation for the other two angles is obtained, i.e., HS $^2\Pi$. Channel 1a in Fig. 4(c) leads to S(^1D), while Fig. 5(b) clearly shows signs of the state crossing involved in the dissociation of the second core-excited state.

B. Potential-energy studies of S+H$_2$

Dissociation through channel 1b can be studied if closing angles are also are considered, see Figs. 6(a)–6(c). Figure 6(a) shows the potential-energy surface for the ground state with respect to the distance between the two hydrogens. In Fig. 6(a) the H_2 distance varies from 4.2 to 1.4 a.u. No dissociation in the direction of channel 1b could be identified. Extending the calculation to a HS distance equal to 10 a.u. and keeping the two hydrogens 1.4 a.u. apart, we obtained S(^1D)+H$_2$(^1S).

The first core-excited state does not show dissociation in the direction of channel 1b, since a small but noticeable potential barrier shows up, see Fig. 6(b). Tunneling through this barrier or excitations of the bending mode may lead to the presence of S+H$_2$ fragments, although one can expect it to be weak. Calculation for HS distance equal to 10 a.u. gives as dissociation products sulfur in the excited $(2p^5 3p^1)^1P$ state and H_2 in the ground state.

Figure 6(c) shows the PES for the second excited state. In this surface we extend the range of HS distances from

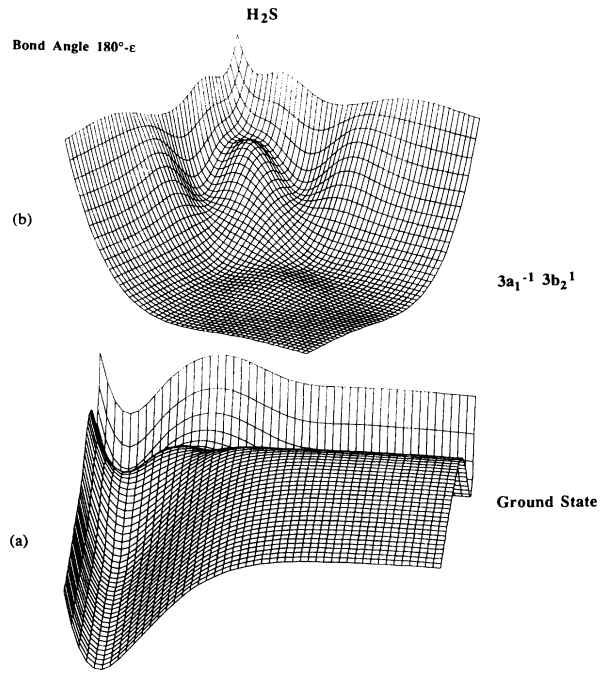

FIG. 5. PES's for the ground and the second core-excited states keeping the H_2S molecule slightly bent. Distortion in the PES indicates the presence of avoided crossing of states.

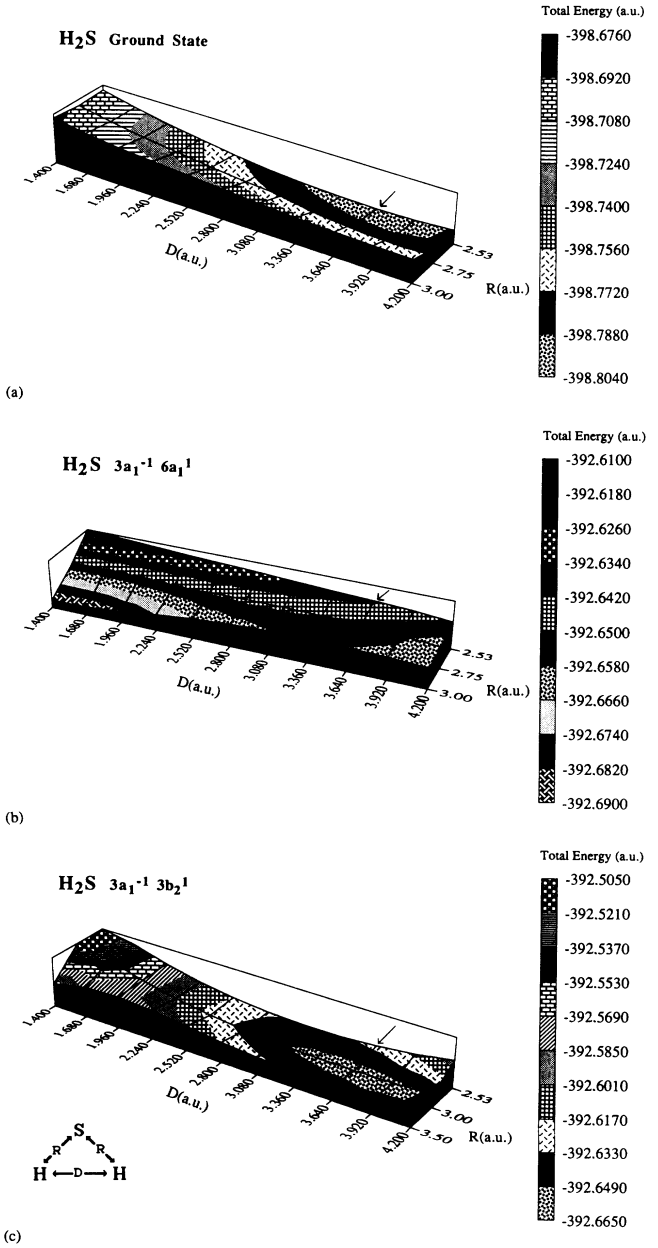

FIG. 6. PES's for the ground state and the two core-excited states in the direction of channel 1b. A small potential barrier is present for $3a_1^{-1}6a_1^1$ through S*+H$_2$ dissociation.

2.53 to 3.5 a.u. The beginning of the dissociation into H_2 can be seen at the HS distance as far as 3.5 a.u. From the figure we clearly see that the second core-excited state is not likely to dissociate via channel 1b in the experimental situation we are addressing. Table I shows the relative dissociative energies of the fragments discussed above. As can be seen in the table the sulfur atom is left in the same state when dissociating along channel 1b as along channel 1a, i.e., a (^1D) state.

C. Crossing of the first and second excited states

Figure 7 shows the potential-energy curve in the direction of channel 2 for the bond angle of 91.96°. An arrow locates the vertical points of excitation. In this region the core-excited state $^1A_1$ is clearly disturbed by the presence of the $^1B_2$ state, something that is effected through vibronic coupling over the antisymmetric stretching mode. Analysis of the natural occupation shows two different situations: one for the molecule with the C_{2v} symmetry, where the $^1A_1$ and $^1B_2$ states do not interact, and another where these two states are part of the same C_s symmetry and do interact. The interaction can be followed by looking at p_x (in-plane) and p_z (in-plane symmetry axis) components in the natural $6a_1$ and $3b_2$ orbitals. A potential search using the ABACUS code was employed for the first excited state. Starting from the ground-state (GS) geometry the curve crossing was hit after four iterations. The bond angle was then 92.79°, the S-H(1) distance 2.634 a.u. and the S-H(2) distance 2.646 a.u. One can infer that in the proximity of the GS equilibrium geometry the molecule dissociates by opening the H-S-H angle while departing from C_{2v} symmetry. The first core-excited state has a contribution from p_z but not p_x in the $6a_1$ orbital at the GS equilibrium geometry, while the second excited state has p_x but no p_z contributions in the $3b_2$ orbital. At the 92.79° bond angle, however, the single occupied orbital in the first core-excited state has $0.18p_x$ and $0.48p_z$, while the second core-excited state, the single occupied orbital, has $0.42p_x$ and $0.42p_z$. The energy separation of the states is only 40 meV at this crossing point.

TABLE I. H_2S dissociation limit (eV) relative to the ground-state minimum energy. (The ground-state total energy at equilibrium geometry is −398.7975 a.u.)

Ground state	
$S(^1D)+H_2(^1S)$	3.91
$S(^3P)+H+H$	6.82
$S(^1D)+H+H$	8.02
$SH(^2\Pi)+H$	3.66
$SH(^2\Sigma^+)+H$	7.79
First core-excited state	
$S^*(^1P)+H_2(^1S)$	164.24
$S^*(^3D)+H+H$	167.81
$SH^*(X\,^2\Sigma^+)+H$	164.32
Second core-excited state	
$S^*(^1D)+H_2(^1S)$	165.99
$S^*(^3P)+H+H$	168.24
$S^*(^1D)+H+H$	170.42
$SH^*(A\,^2\Pi)+H$	171.49
$SH^*(B\,^2\Sigma^+)+H$	175.81

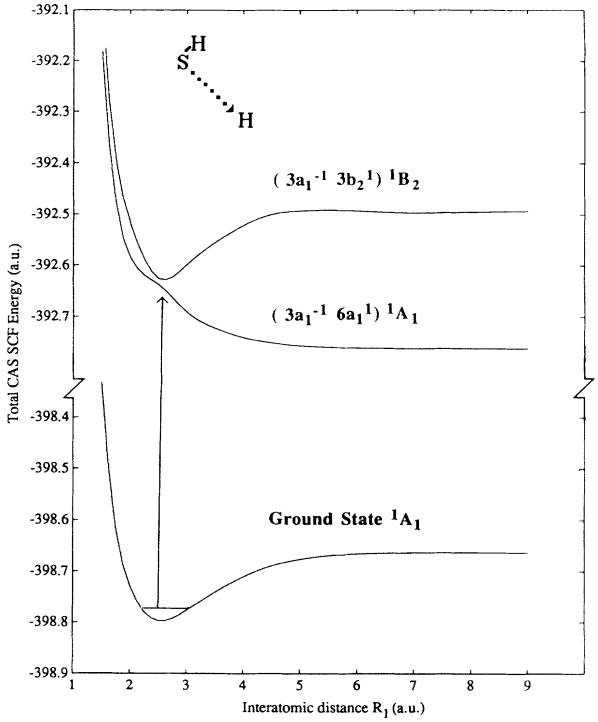

FIG. 7. Potential-energy curve in the direction of channel 2. Crossing between $3a_1^{-1}6a_1^1$ and $3a_1^{-1}3b_2^1$ close to the equilibrium position is indicated. See discussion in the text.

Taking into consideration (1) the behavior of the curves shown in Fig. 7, (2) the natural orbital occupations, and (3) the small energy difference, one can conclude that the first and second excited states will interact in the direction of channel 2. The dissociation thus occurs through an avoided crossing. This behavior is similar, but not identical, to uv photodissociation of several first- and second-row hydrides. In these cases the first excited states often predissociate through an avoided crossing also involving a mixed valence Rydberg transformation [13,14].

D. Dissociation to HS^*+H, S^*+H_2, and S^*+H+H

In this section we proceed with the analysis of the H_2S energy surfaces shown in Figs. 2–5 by looking at the potential-energy curves resulting from the intersection between these surfaces and planes through channel 1a or channel 2. For the same state different interatomic bond angles are plotted.

1. Ground $^1A_1$ state

Figure 8(a) shows the ground-state curves at four different interatomic angles, 91.96°, 135°, 180°−ϵ, and

180°, in the direction of channel 1a. The dissociation limits are also indicated. Apart from the discussion we carried out previously, one can compare the dissociation limits given in Table I for $S(^3P)+[H+H](^3S)$ and $S(^1D)+[H+H](^1S)$. From optical reference data [15] the energy differences between ^3P to ^1D and ^1D to ^1S are 1.14 and 2.75 eV, respectively, while the difference between our two calculated limits is 1.19 eV. Our calculated value thus agrees well with the experimental results.

Figure 8(b) shows the same type of data as 8(a) but now the intersection is in the direction of channel 2. At $180°-\epsilon$ a potential barrier around 3.5 a.u. shows up as a result of an avoided crossing. The potential well in the direction of channel 2 is more shallow than in the direction of channel 1a, which is the obvious result that dissociation of one hydrogen is less costly than dissociation of both. The dissociation energies are given in Table I.

2. *Core-excited $^1A_1$ state*

The potential curves in the direction of channel 1a for the first core-excited state are plotted in Fig. 9(a). The equilibrium geometry in this direction is at 180° rather than at 91.96°, and excitation from the ground state leads to a linear configuration with a prolonged SH bond. Channel 1a is thus energetically preferred over channel 1b. The total energy at the vertical excitation point is 0.27 eV lower than the dissociation energy, which indicates that dissociation via vertical excitation is not possible. However, if the full Franck-Condon region is taken into account dissociation can occur. Indeed if one adds the ground-state zero vibrational energy, about 0.84 eV [16], to its potential curve a Franck-Condon region of the length of about 0.64 a.u. is covered in the S+H+H directions. Using the potential curve at the equilibrium bond angle, the turning point ($R=2.27$ a.u.) hits the PES of the excited state 1.08 eV above the dissociation limit. Thus dissociation can occur although with rather small probability since the major part of the vibrational states will end up within the nondissociative region.

Figure 9(b) shows the potential-energy curve of the $^1A_1$ state in the direction of channel 2. As in Fig. 9(a) the total energy is lower at 180°, since the excitation populates an angle antibonding orbital. The bond angle will open while the molecule dissociates. It is clear that the vibronic interaction between $^1A_1$ and $^1B_2$ states perturbs the $^1A_1$ state strongly at 91.96° around 2.5 a.u., moderately at 135° around 3.0 a.u., but only slightly at 180°.

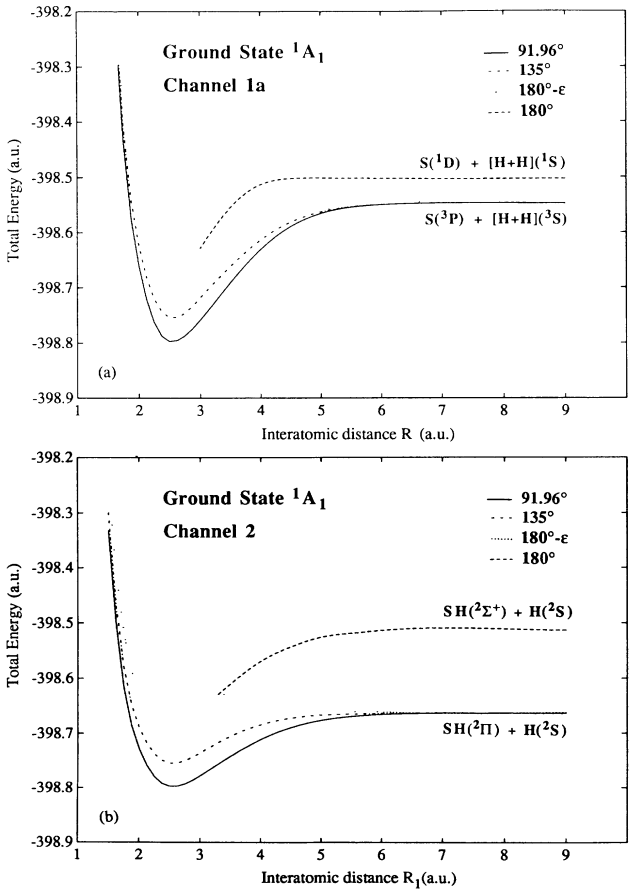

FIG. 8. Potential-energy curve for the ground state in directions of channels 1a and 2. The dissociation products are indicated.

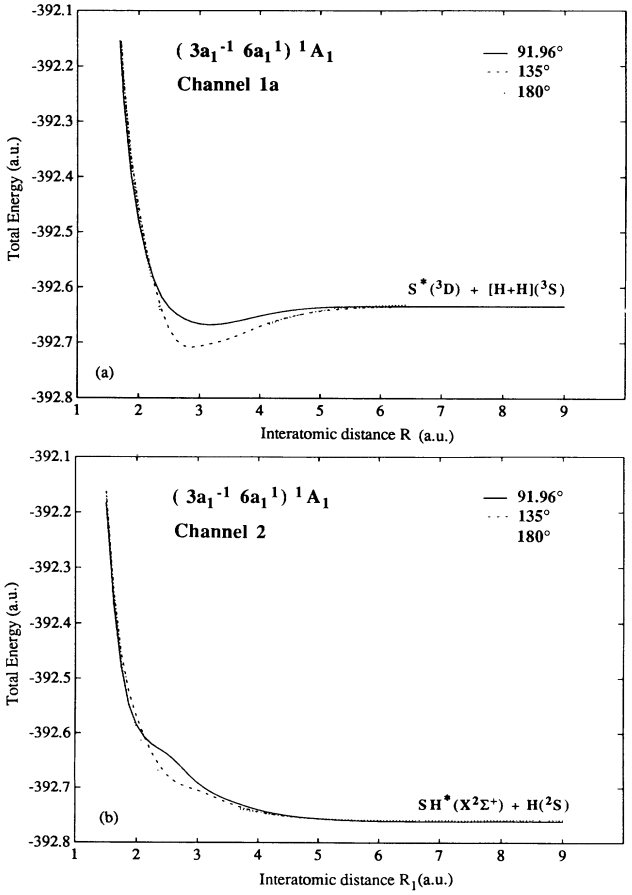

FIG. 9. Potential-energy curve for the H_2S^* $^1A_1$ state in the directions of channels 1a and 2. The dissociation products are indicated.

TABLE II. Theoretical and experimental HS resonant Auger energies. Parentheses in column four denote experimental error.

State	Dominant configuration	Theoretical	Experimental[a]
$^3\Sigma^-(p_{1/2})$	$(5\sigma^2;2\pi^2)$	151.59	149.3(3)
$^3\Sigma^-(p_{3/2})$	$(5\sigma^2;2\pi^2)$	150.34	148.1(3)
$^1\Delta(p_{1/2})$	$(5\sigma^2;2\pi^2)$	150.14	148.1(3)
$^1\Sigma^+(p_{1/2})$	$(5\sigma^2;2\pi^2)$	149.00	147.2(3)
$^1\Delta(p_{3/2})$	$(5\sigma^2;2\pi^2)$	148.89	147.0(3)
$^1\Sigma^+(p_{3/2})$	$(5\sigma^2;2\pi^2)$	147.75	146.0(3)
$^3\Pi(p_{1/2})$	$(5\sigma^1;2\pi^3)$	147.65	145.3(6)
$^1\Pi(p_{1/2})$	$(5\sigma^1;2\pi^3)$	146.36	144.3(6)
$^3\Pi(p_{3/2})$	$(5\sigma^1;2\pi^3)$	146.40	144.1(3)
$^1\Pi(p_{3/2})$	$(5\sigma^1;2\pi^3)$	145.11	143.1(3)
$^1\Sigma^+(p_{1/2})$	$(5\sigma^0;2\pi^4)$	141.15	
$^1\Sigma^+(p_{3/2})$	$(5\sigma^0;2\pi^4)$	139.90	

[a]Values taken from paper I.

3. *Core-excited $^1B_2$ state*

Figures 10(a) and 10(b) show the potential curves for the second excited in the directions of channels 1a and 2, respectively. The dissociation energy of $S^*(^3P)+[H+H](^3S)$ is given in Table I. At the bond angle of 180° the dissociation leads to $S^*(^1D)+[H+H](^3S)$. The energy minimum is at 91.96°. At this angle there is a shallow potential well, which contains only one vibrational level (of ground-state frequency). Vertical excitation from the ground state will still lie below the dissociation energy. However, taking into account the Franck-Condon region, which extends from 2.27 to 2.91 a.u. for a fixed equilibrium bond angle, dissociation may also occur. From 2.27 up to 2.44 a.u. at 91.96° the potential energy is also higher than the dissociation limit, see Table I.

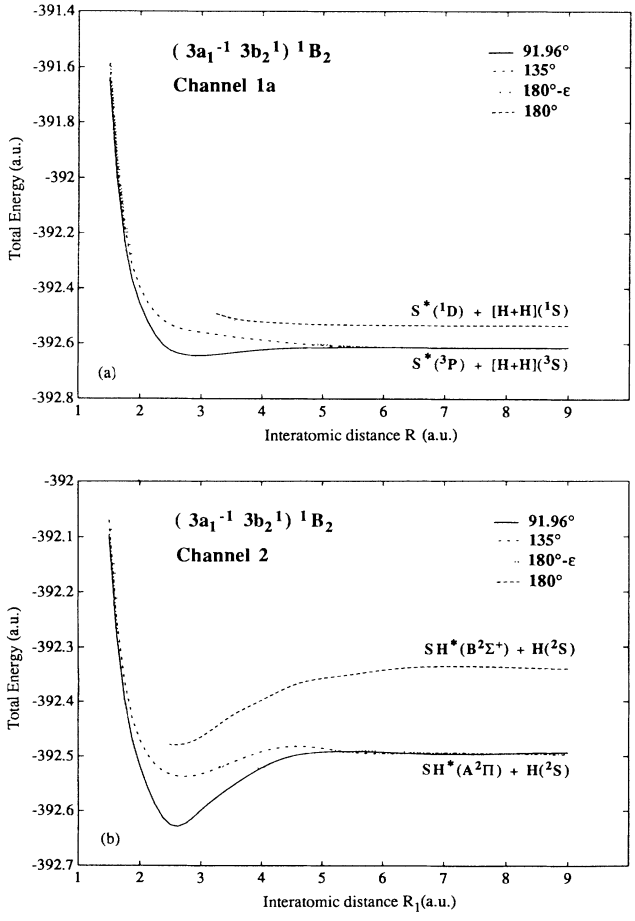

FIG. 10. Potential-energy curve for the H_2S^* $^1B_2$ state in the directions of channels 1a and 2. The dissociation products are indicated.

A necessary condition for a line spectrum is that the PES for the core-excited state be parallel to the PES for the appropriate final electronic state, otherwise a superposition of spectra is obtained, which blurs any spectral structure. The PES's for the final state have not been calculated, and therefore are an appropriate subject for a future study. We have, however, performed a simple semiclassical estimate of the dissociation length in H_2S using the numerical values of the potential energy in the direction of channel 2 from the curve shown in Fig. 9(b). A dissociation of length 3.9 a.u. was obtained for a lifetime of 5.5 fs. The lifetime of the $2p$ core hole of the isoelectronic argon atom was used as an approximation for the lifetime of the $2p$ core hole in H_2S. For a polyatomic molecule, however, the excess energy is distributed between internal (rotation and vibrational) and external (translational) degrees of freedom, and this division should rather be obtained quantum mechanically. Furthermore, the initial conditions with a Franck-Condon distribution of momenta from the ground state projected on the final state by excitation has an influence on the dissociation length.

Channels 1 and 3 were considered on experimental grounds in paper I. Channel 1 was ruled out because no Auger lines from free sulfur atoms were observed at the relevant energy region (as predicted by MC Dirac-Fock calculations). Some extra faint structures on the high-energy side of the spectrum were attributed to resonant Auger from core-excited H_2S (channel 3). This attribu-

TABLE III. Energy differences for HS resonant Auger energies using different approximation together with the experimental values.

States	Theoretical differences (4221)[a] (eV)	Theoretical differences (5331) (eV)	Experimental differences ($P_{1/2}$) (eV)	Experimental differences ($p_{3/2}$) (eV)
$^3\Sigma^-$-$^1\Delta$	1.45	1.47	1.2	1.1
$^1\Delta$-$^1\Sigma^+$	1.14	1.09	0.9	1.0
$^1\Sigma^+$-$^3\Pi$	1.35	1.37	1.9	1.9
$^3\Pi$-$^1\Pi$	1.28	1.31	1	1
$^1\Pi$-$^1\Sigma^+$	5.22	5.08		

[a]The numbers refer to the size of the active space following the orbital ordering (a_1,b_2,b_1,a_2).

tion is based on the fact that participator decay ends up in normal photoelectron states, while spectator decay ends up in photoelectron satellite states, thus being known from the photoelectron spectrum of H_2S.

E. Electronic decay channels for HS*

According to the PES calculations the dissociation of one hydrogen after core excitation is the major decay channel. In order to determine whether some of the lines in the experimental spectra come from decay in the HS* fragment after dissociation, we present here calculations of the resonant Auger energies, see Table II. Such nonradiative transitions would take place from the initial excited configuration $1\sigma^2 2\sigma^2 3\sigma^1 1\pi^4 4\sigma^2 5\sigma^2 2\pi^4$ to the final two-hole configurations $5\sigma^0 2\pi^4$, $5\sigma^1 2\pi^3$, or $5\sigma^2 2\pi^2$. Six possible electronic states are in $\Lambda\Sigma$ coupling related to these final-state configurations: $(5\sigma^2 2\pi^2)^3\Sigma^-$, $(5\sigma^2 2\pi^2)^1\Delta$, $(5\sigma^2 2\pi^2)^1\Sigma^+$, $(5\sigma^1 2\pi^3)^3\Pi$, $(5\sigma^1 2\pi^3)^1\Pi$, and $(5\sigma^0 2\pi^4)^1\Sigma^+$. By comparing with the normal Auger spectrum of HCl [17,18], which represents the same final configuration states as the spectrum of HS*, some peaks ($a-e$ and g) were tentatively identified in paper I to correspond the transitions to the final states $(5\sigma^2 2\pi^2)^3\Sigma^-$, $(5\sigma^2 2\pi^2)^1\Delta$, $(5\sigma^2 2\pi^2)^1\Sigma^+$, $(5\sigma^1 2\pi^3)^3\Pi$, $(5\sigma^1 2\pi^3)^1\Pi$, and $(5\sigma^2 2\pi^4)^1\Sigma^+$ of HS*, respectively. Thus already from these considerations based on analogy it seems that the main decay channel of the core-excited H_2S is the dissociation of one hydrogen atom followed by the Auger process in the core-excited HS molecule, referred to as channel 2 in the Introduction.

However, an even stronger indication is given by the results of the MCSCF calculations. Table II shows the results of these calculations together with an assignment of the experimental spectra. The absolute Auger energies are consistently 1.8 to 2.3 eV too large. This error, typical for MCSCF calculations of Auger transition energies, results mainly from neglect of the dynamical correlation of the two valence electrons that are missing in the final states. The differences between peak positions are shown in Table III. The experimental spin-orbital splitting of 1.25 eV has been assumed to separate computed states of identical spin and spatial symmetry. With the experimental assignment adopted in this table a good experimental agreement can be obtained. The assignments are further supported by column 2 in this table which shows yet another calculation using a larger active space, but which changes the computed energy differences only little. Thus, from pure energetic grounds it can be inferred that the main features of the resonance Auger spectrum of H_2S to a large extent results from decay of the core-excited HS species.

IV. SUMMARY

MCSCF calculations of the potential-energy surfaces of the core-excited states of H_2S indicate the existence of a dissociative channel leading to core-excited HS. We find that calculations of the HS resonance Auger energies can well be used to interpret the experimental results. We thus conclude that the main decay channel of the excited states resulting from resonant $3a_1 \rightarrow 6a_1$ and $3a_1 \rightarrow 3b_2$ excitations is the dissociation of one hydrogen atom followed by the Auger decay in core-excited HS. The vertical excitation region of the $(3a_1^{-1}3b_2^1)^1B_2$ state is close to a crossing between this state and the $(3a_1^{-1}6a_1^1)^1A_1$ state. The presence of this crossing will then lead to the dissociation of one hydrogen also following the $3a_1 \rightarrow 3b_2$ excitation.

Taking into consideration the Franck-Condon region the PES analysis indicates that one may also have dissociation of both hydrogens followed by the Auger decay in the excited sulfur atom. Dissociation of both hydrogens into separated atoms can lead to core-excited free sulfur in the ^3D state upon $3a_1 \rightarrow 6a_1$ and ^3P upon $3a_1 \rightarrow 2b_2$ excitation. On the other hand, dissociation of the hydrogen molecule would lead to free sulfur in the ^1P state. Even though the potential-energy calculation indicates the possibility of dissociation to free sulfur, the measured electron spectra do not indicate structures arising from the decay of core-excited sulfur (paper I). Since the potential is bound toward double hydrogen dissociation and since the limits of the Franck-Condon region only give moderate excess energy, one can expect diffuse contributions from superposition of "dissociative molecular"

spectra with varying energies along this channel. The third possible event, namely, resonance Auger decay in H_2S, was on experimental grounds predicted to make a weak contribution to the observed spectrum (Aksela *et al.*, paper I). The theoretical account of the relative probabilities of these possible events has to await results from time-dependent quantum calculations for all species and states involved.

ACKNOWLEDGMENTS

We acknowledge CNPq of Brazil (A.N.B.) and the Swedish Natural Science Research Council (H.Å.) for financial support. We also acknowledge H. Aksela, N. Correia, and A. Cesar for valuable discussions. H. Ollaiver is acknowleged for providing technical support.

[1] P. Morin and I. Nenner, Phys. Rev. Lett. **56**, 1913 (1986).
[2] H. Aksela, S. Aksela, M. Ala-Korpela, O. P. Sairanen, M. Hotokka, G. M. Bancroft, K. H. Tan, and J. Tulkki, Phys. Rev. A **41**, 6000 (1990).
[3] H. Aksela, S. Aksela, A. Naves de Brito, G. M. Bancroft, and K. H. Tan, preceding paper, Phys. Rev. A **45**, 7948 (1992).
[4] N. E. Henriksen, J. Zhang, and G. G. Imre, J. Chem. Phys. **89**, 5607 (1988).
[5] A. Cesar, and H. Ågren (unpublished).
[6] H. J. Aa. Jensen, and H. Ågren, Chem. Phys. Lett. **110**, 140 (1984).
[7] T. U. Helgaker, H. J. Aa. Jensen, and P. Jørgensen, J. Chem. Phys. **84**, 6280 (1986).
[8] A. Cesar, H. Ågren, A. Naves de Brito, S. Svensson, L. Karlsson, M. P. Keane, B. Wannberg, P. Baltzer, P. G. Fournier, and J. Fournier, J. Chem. Phys. **93**, 918 (1990).
[9] J. G. Hayes, in *Fitting Data in More than one Variable,* edited by J. G. Hayes (Athlone, London, 1970), Chap. 7.
[10] B. O. Roos, and P. Siegbahn, Theor. Chim. Acta **17**, 199 (1970).
[11] A. Strömberg, U. Wahlgren, L. Pettersson, and P. Siegbahn, Chem. Phys. **89**, 323 (1984).
[12] E. Magnusson and H. F. Schaefer III, J. Chem. Phys. **83**, 5721 (1985).
[13] S. Canuto, J. Phys. B **12**, 3149 (1979).
[14] J. Müller, H. Ågren, and S. Canuto, J. Chem. Phys. **76**, 5067 (1982).
[15] E. M. Charlotte, *Atomic Energy Levels,* Natl. Bur. Stand. Ref. Data Ser., Nat. Bur. Stand. (U.S.) (U.S. GPO, Washington, D.C., 1952), Vol. I.
[16] I. M. Mills, *Specialist Reports Theoretical Chemistry* (The Chemical Society, London, 1974), Vol. 1.
[17] H. Aksela, S. Aksela, M. Hotokka, and M. Jäntti, Phys. Rev. A **28**, 287 (1983).
[18] O. M. Kvalheim, Chem. Phys. Lett **98**, 457 (1983).

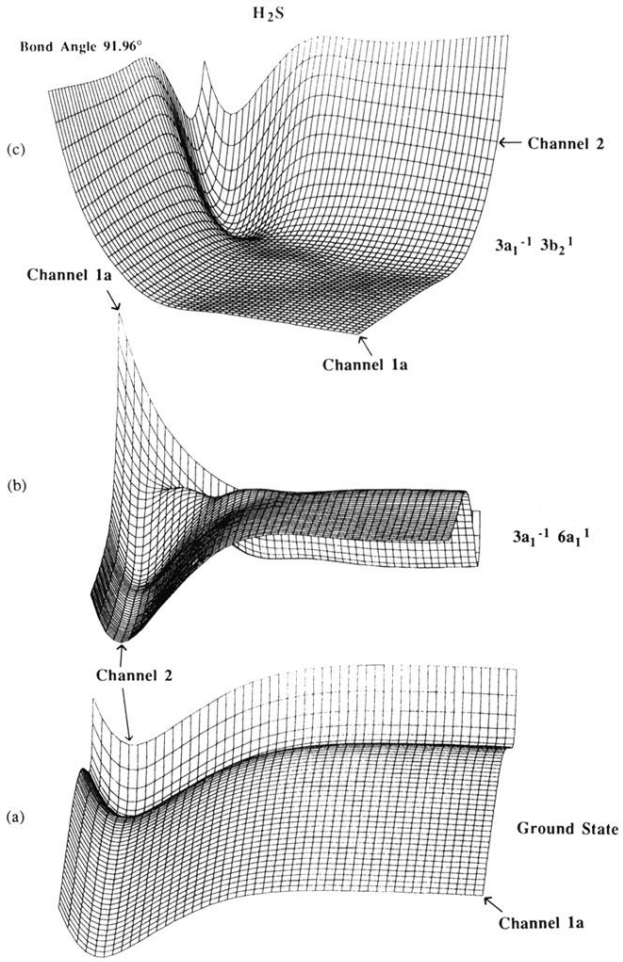

FIG. 2. Graphical representations of the PES's for the ground state, first, and second core-excited states at the equilibrium bond angle. Channels 2 and 1a are indicated. The strong dissociative character of H_2S in the $3a_1^{-1}6a_1^{1}$ state provides the condition for a fast dissociation into $HS^* + H$ before the Auger decay. See text for futher discussion.

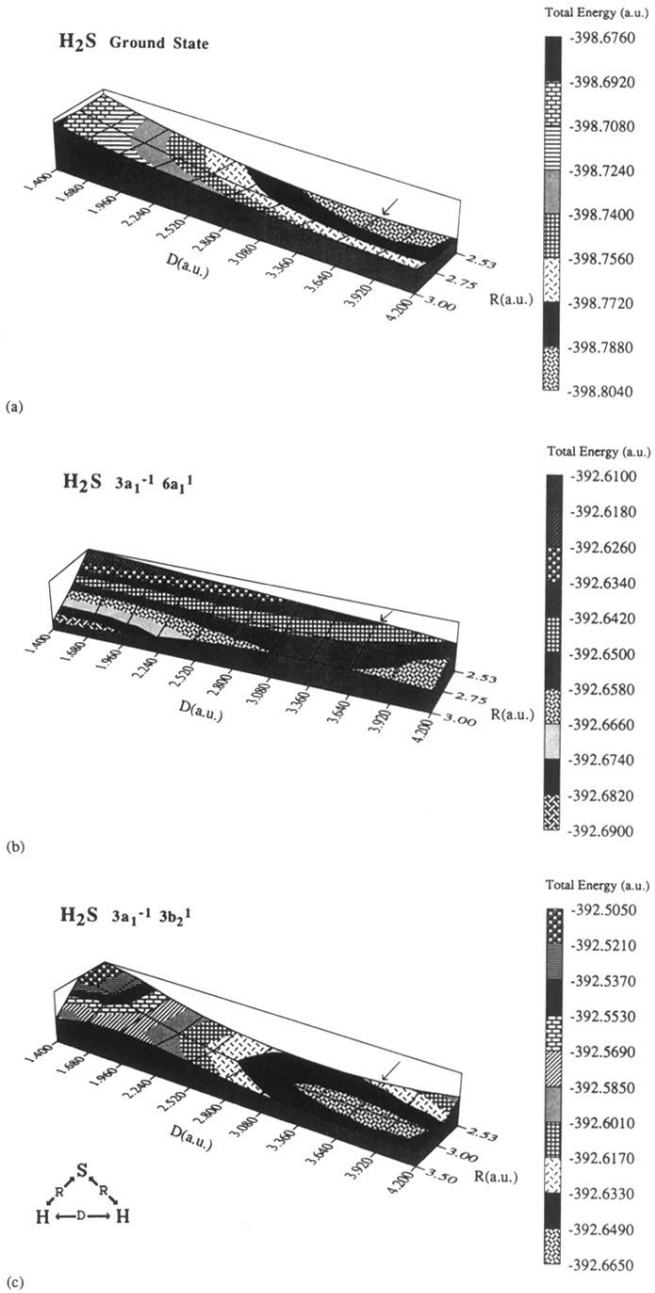

FIG. 6. PES's for the ground state and the two core-excited states in the direction of channel 1b. A small potential barrier is present for $3a_1^{-1}6a_1^1$ through $S^* + H_2$ dissociation.